Review

Lessons from the use of in vivo cellular calcium imaging in primary sensory neurons and spinal cord

The Neuroscientist I–20

© The Author(s) 2025



Article reuse guidelines: sagepub.com/journals-permissions DOI: 10.1177/10738584251360724 journals.sagepub.com/home/nro



John Shannonhouse¹, Yan Zhang¹, Hyeonwi Son¹, Eungyung Kim¹, Deoksoo Han¹, Joon Tae Park², and Yu Shin Kim^{1,3}

Abstract

Primary somatosensory neurons, glial cells in the peripheral ganglia, and neural circuits in the spinal cord function as dynamic network circuits that transmit information to the brain. Although a variety of methods and techniques have been used to study individual neurons or tissue explants, the number of neurons that can be monitored is limited. Imaging intact primary sensory neurons, such as those in the dorsal root ganglion and trigeminal ganglia, and the spinal cord in vivo using fluorescent calcium markers helps overcome the limitations of previous methods and techniques by allowing researchers to monitor tens to thousands of cells simultaneously. This allows researchers to conduct experiments to elucidate somatosensory mechanisms and responses to axonal injury that were previously difficult or impossible to observe. Using this approach, researchers have studied dynamic neural network circuits, connectivity, responses to soft and deep touch, heat, cold, chemicals, inflammation, and injury, and they have repeatedly imaged individual neurons over long periods of time. Approaches include using calcium-sensitive fluorescent dyes and genetically encoded markers, performing terminal exposure surgeries, using chambers designed to monitor large numbers of cells or repeatedly imaging small numbers of cells, and imaging animals with or without anesthesia. This review discusses the advantages and disadvantages of in vivo calcium imaging for studying somatosensory and axonal injury in peripheral sensory ganglia and the dorsal spinal cord, as well as anticipated future directions.

Keywords

primary sensory neurons, dorsal root ganglia, trigeminal ganglia, spinal cord, in vivo GCaMP calcium imaging

Introduction

The somatosensory system monitors all types of somatosensory sensations, including soft and deep touch, proprioception, pain, itch, hot and cold, and chemical stimuli. Somatosensory functions as an ensemble of networks to discriminate between painful and nonpainful sensations (Ropero Peláez and Taniguchi 2016) or fine tactile discriminations (Johansson and Flanagan 2009). Primary sensory neurons in the peripheral ganglia innervate peripheral targets and transmit action potentials to the spinal cord and brain. To better understand these networks and circuit activity or patterns under normal conditions and how these networks respond to damage, researchers must use methods that study neurons, glial cells, and other cell types and dynamic network circuits at the population level. Explants can be useful for studying the function of individual neurons and local networks, but they have the obvious limitation that they often do not innervate targets in the brain, spinal cord, or skin, although some explants include many relevant tissues (Fadaka and others 2025). Ultimately, we want to understand how stimuli from the skin and underlying tissues reach the brain and are interpreted there, so it is desirable to study intact sensory ganglia and nuclei in their normal anatomical and physiological context.

In vivo neural firing is essential for somatosensation, but until recently, tools for studying it have been limited to a relatively small number of cells. To overcome this,

¹Department of Oral & Maxillofacial Surgery, School of Dentistry, University of Texas Health Science Center at San Antonio, TX, USA ²Division of Life Sciences, College of Life Sciences and Bioengineering, Incheon National University, Incheon, South Korea ³Programs in Integrated Biomedical Sciences & Translational Sciences, University of Texas Health Science Center at San Antonio, TX, USA

Current Affiliation: John Shannonhouse, Yan Zhang, Hyeonwi Son, Eungyung Kim, Deoksoo Han, Joon Tae Park and Yu Shin Kim is now affiliated with Department of Endodontics, School of Dentistry, University of Alabama at Birmingham, Birmingham, AL, USA.

Corresponding Author:

Yu Shin Kim, Department of Oral & Maxillofacial Surgery, University of Texas Health at San Antonio, 7703 Floyd Curl Drive, San Antonio, TX 78229, USA.

Email: kimy I @uthscsa.edu

imaging based on changes in cytosolic calcium dynamics has been developed. Fluorescent calcium-sensitive indicators respond in neurons that normally have low cytosolic calcium levels. Their activity increases as cytosolic Ca²⁺ concentration increases in proportion to action potential frequency (Chisholm and others 2018; Helmchen and others 1996). In vivo calcium imaging has two major advantages over electrophysiological approaches (Anderson and others 2018). Calcium imaging allows simultaneous analysis of tens, hundreds, or thousands of neurons. Furthermore, it can be used to image repeatedly over long periods of time with appropriate surgical preparation, allowing researchers to observe physiological changes in the same cell or multiple cells over time. Thus, it has a wide range of applications: numerical population response analysis where a few vs tens vs up to hundreds of neurons respond under different conditions; studying the morphology of neuronal subtypes and their response patterns to specific stimuli; observing changes in neuronal morphology and response patterns under specific conditions, such as injury, drug treatment, or mutation; observing changes in neuronal sensitivity to stimuli; studying calcium signaling responses in unexcited cells or under conditions where neurons are not firing; and observing changes in neurons over time at the individual neuron and population level. In vivo Ca²⁺ imaging is emerging as a powerful tool, useful for studying neurons from many parts of the nervous system. This article reviews, as an example, the many ways that Ca²⁺ imaging has provided new information about primary sensory neurons and the spinal cord. This review also discusses the shortcomings of this technique, such as its limitations in imaging cells near the surface due to limitations in the depth to which the excited and emitted light can penetrate the tissue, not being able to measure action potentials directly, and low temporal resolution.

Spinal Cord Imaging

Spinal cord imaging is useful for linking specific somatosensory inputs to patterns of neural activity and for studying axonal damage. Layers I–IV of the dorsal horn (DH) of the spinal cord receive somatosensory inputs from primary sensory neurons and send action potentials to the brain. The location of the dorsal horn is ideal for exposure surgery. Layers I–IV are close enough to the surface to allow calcium imaging of neurons and other cell types in vivo using fluorescence microscopy. Similarly, the dorsal root fiber pathways of primary sensory neurons can be directly exposed and imaged. Results from DH imaging show great promise for studying somatosensory networks and circuits (Chen and others 2018; Johannssen and Helmchen 2010; Nishida and others 2014; Ran and others 2016; Sekiguchi and others 2016; Shekhtmeyster and

others 2023a; Yoshihara and others 2018). For example, calcium imaging models of network activity have shown that different stimuli activate different neuronal subpopulations (Farrar and others 2012; Johannssen and Helmchen 2010; Lorenzana and others 2015; Nishida and others 2014; Ran and others 2016; Sekiguchi and others 2016; Yoshihara and others 2018). Moreover, tens (Chen and others 2018; Johannssen and Helmchen 2010; Sekiguchi and others 2016; Tang and others 2015; Yoshihara and others 2018) to hundreds (Farrar and others 2012; Nishida and others 2014; Ran and others 2016; Shekhtmeyster and others 2023a) and even thousands (Shekhtmeyster and others 2023b) of neurons or glial cells were monitored to identify meaningful patterns in network activity. There are two main approaches to imaging calcium activity in DH cells and dorsal root fibers: loading the cells with calcium-sensitive fluorescent dyes and expressing calcium-sensitive fluorescent proteins in the cells of interest.

Spinal Cord Imaging Using Calcium-Sensitive Fluorescent Dyes

A significant advantage of calcium-sensitive fluorescent dyes over genetically encoded calcium indicators is that they can be used in any strain, species, or cell type, provided the dye can be loaded and the cells examined by fluorescence microscopy. The calcium-sensitive fluorescent dye Oregon Green 488 BAPTA-1AM has been loaded into dorsal horn cells after spinal transection to image calcium influx and dynamics among a variety of cell types (Ikeda and others 2006; Johannssen and Helmchen 2010; Ran and others 2016). Early experiments imaging spinal muscle fibers showed that in vivo calcium gradients closely follow recorded action potentials (Ikeda and others 2006). Furthermore, it has been shown that electrical stimulation of afferent nerves activates DH neurons broadly, but only a small, distinct subpopulation responds to mechanical stimulation, demonstrating that in vivo calcium imaging can be used to map neural networks in real time (Johannssen and Helmchen 2010). Improvements in animal restraint and movement stabilization have made it easier to map neural networks in real time. Systems capable of imaging ~400 DH neurons at a time have shown a series of overlapping neuronal populations that respond to a wide range of temperatures, from noxious hot to noxious cold, with temperature activation thresholds evenly distributed across the entire temperature range, and with formalin and oxaliplatin affecting warm, cold, and multimodal neurons differently (Ran and others 2016; Ran and others 2021). Analyzing coding populations of this scale would be impossible using conventional electrophysiology. However, calcium-sensitive dyes have several

major drawbacks: they do not label specific cell types, so unless neurons are clearly identified during image analysis, the types of neuronal subtype data that can be collected are severely limited. Neurons analyzed were mostly in the superficial laminae. Moreover, the dye is rapidly inactivated, and loading it can cause tissue damage (Xu and Dong 2019).

Spinal Cord Imaging Using Genetically Encoded Calcium Indicators

Transgenic or vector-delivered fluorescent genetically encoded calcium indicators (GECIs) can be used to label specific cell types using cell type-specific promoters or Cre conditional promoters and cell type–specific Cre. Compared with calcium-sensitive dyes, the expressed proteins have the advantage of being longer-lasting during imaging without signal loss and of not requiring cell staining immediately before imaging. Many studies have used this approach to image the mouse brain in vivo (Cheng and others 2019). However, less work has been done using this approach to image the spinal cord in vivo (Cheng and others 2019). A pioneering study using plasmid-encoded Yellow Chameleon monitored the activity of ~200 L1 DH neurons in response to mechanical and thermal stimuli and distinguished between innocuous and noxious coding in layers I-III of the dorsal horn (Nishida and others 2014). Using adeno-associated virus (AAV) delivered GCaMP6, researchers have shown that approximately half of the mechanosensory neurons in laminae I–II are potentiated by norepinephrine afferents descending from the locus coeruleus (Chen and others 2018; Kawanabe and others 2021; Kohro and others 2020), which would have been difficult or impossible to achieve using electrophysiology. Similarly, DH astrocytes studied at the population level using AAV-delivered GCaMP have been shown to respond to noxious stimuli in both superficial and deep laminae, but not to innocuous stimuli (Sekiguchi and others 2016; Shekhtmeyster and others 2023a; Shekhtmeyster and others 2023b; Yoshihara and others 2018). At the population level, it has been possible to monitor a variety of signaling patterns in different cell types, including the coordination of inhibitory and excitatory DH neurons (Sullivan and Sdrulla 2022) and calcium activity patterns in astrocytes and microglia (Rieder and others 2022). However, analysis was largely confined to the surface laminae.

Repetitive Imaging on Mice without Anesthesia

Traditional real-time imaging methods require terminal exposure surgery and often necessitate that the mouse be anesthetized during imaging. These limitations make repeated imaging impossible and raise questions about how similar the observed neural activity patterns are to those in awake, behaving animals. To resolve these limitations, the implantation of viewing chambers or microprisms has been proposed. These can be inserted through appropriate surgical preparation, allowing repeated measurements of spinal cell activity over several days or weeks without anesthesia. These imaging methods revealed that in freely moving animals, a small number of DH neurons respond to specific stimuli, whereas astrocytes respond only to large-scale inflammation. This method also found that the frequency and amplitude of spontaneous neuronal activity and the activity evoked by mechanical pinch stimulation were greater in freely moving mice than in anesthetized mice. However, only a small number of cells could be imaged in this method (Tables 1 and 2) (Sekiguchi and others 2016; Shekhtmeyster and others 2023a; Shekhtmeyster and others 2023b).

Studying Axonal Injury Using Repetitive Imaging Fluorescence Microscopy

Fluorescent labeling has been used to study degeneration and regeneration of superficial axons after spinal cord injury. This can range from studying interactions of specific cell types through genetic encoding to studying interactions with blood vessels and immune cells. Early experiments used green fluorescent protein (GFP) expressed from a neuron-specific promoter to repeatedly image identical axons in the spinal cord and characterize differences in degeneration and stability of axons proximal and distal to the injury site (Kerschensteiner and others 2005). Simultaneous imaging of blood vessels and neurons showed that axonal regeneration did not correlate with blood vessel location (Dray and others 2009). Microglial scar formation and axonal degeneration were observed over a five-week period after focal spinal cord injury (Farrar and others 2012). Imaging of yellow fluorescent protein (YFP)-labeled axons and GFP-labeled macrophages and microglia allowed morphological distinction between microglia and macrophages, demonstrating differences in their roles in axonal degeneration (Evans and others 2014; Wu and others 2024). Using repetitive imaging of individual axons as they branch, it was possible to show that retrograde degeneration of severed axons stops at the point of branching (Lorenzana and others 2015). The timing of calcium release after injury can also be studied to determine the effect on axon populations (Orem and others 2020). Such detailed mapping of individual axon degeneration and regeneration, the site of injury, and interactions with other cell types can only be achieved using repetitive imaging using stable, long-term, cell type-specific fluorescent markers.

Table 1. In Vivo Spinal Cord Calcium Imaging Studies.

-			
Imaged Area	Fluorophore	Number of Cells Imaged per Animal	Reference
Spinal dorsal horn laminae I-VII	AAV-delivered GCaMP7f or GCaMP6f in GFAP $^+$ or TacR I $^+$ cells	Up to $>$ 100 astrocytes or $>$ 100 neurons per trial in freely moving mice	Shekhtmeyster and others (2023a, 2023b)
Dorsal white matter tracts	Transgenic GCaMP3 in GFAP $^+$ or CX $_3$ CR $_1^+$ cells	Up to five region of interest (ROIs) (astroglia or microglia) per square micron	Rieder and others (2022)
Spinal dorsal horn	Transgenic GCaMP6s in vGluT2 ⁺ or vIAAT ⁺ neurons	Up to ~30 neurons	Sullivan and Sdrulla (2022)
Spinal dorsal horn	Oregon Green 488 BAPTA-1	~300 neurons	Ran and others (2021)
Dorsal column axons	Transgenic GCaMP6f in Advil + neurons	Up to ∼70 axons	Orem and others (2020)
Spinal dorsal horn	GCaMP6m via AAV in He5 ⁺ astrocytes	Up to ∼40 astrocytes	Kohro and others (2020)
Spinal dorsal horn	GCaMP6 via AAV with gfaABC ₁ D promoter	>20 astrocytes	Yoshihara and others (2018)
Spinal dorsal horn	GCaMP6 via AAV with synapsin promoter	>80 neurons	Chen and others (2018)
Spinal dorsal horn	Oregon Green 488 BAPTA-I	~400 neurons	Ran and others (2016)
Spinal dorsal horn	GCaMP6 via AAV with either CaMKII or	>15 neurons or $>$ 20 astrocytes in freely moving	Sekiguchi and others (2016)
	GfaABC _I D promoters	mice	
Spinal dorsal funiculus	Transgenic GCaMP with Thy! promoter	15–20 axons	Tang and others (2015)
Spinal dorsal horn	Yellow Chameleon plasmid with CAG	>200 neurons	Nishida and others (2014)
	promoter via in utero electroporation		
Spinal afferents from DRG, spinal dorsal horn	Transgenic YFP with Thy1 promoter; transgenic GFP with CX3CR1 promoter	~10 axons; >100 microglia	Farrar and others (2012)
Spinal dorsal horn	Oregon Green 488 BAPTA-1	~25 neurons	Johannsson and Helmchen (2010)
Spinal dorsal horn	Oregon Green 488 BAPTA-1	~7 neurons	lkeda and others (2006)

Imaging Studies.
Calcium
ory Ganglia C
Sensory
Peripheral
In Vivo
le 2.
Tab

ganglion oot ganglion te and petrosal	riuoropnore	Number of Cells Imaged per Animal	Kererence
lion etrosal			
	Transgenic GCaMP6 with Cre-inducible promoter	Total neurons visualized per animal not described	Huerta and others (2023)
	Transgenic GCaMP3 with Pirt promoter	Total neurons visualized per animal not described	Iseppon and others (2023)
ganglia	Transgenic GCaMP6s with Snap25 promoter	Total neurons visualized per animal not described	Fowler and others (2022)
Dorsal root ganglion Transgeni	Transgenic GCaMP6 with Pirt promoter	~1600 neurons	Zheng and others (2022)
Dorsal root ganglion Transgeni	Transgenic GCaMP3 with Pirt promoter	Total neurons visualized per animal not described	MacDonald and others (2021)
Dorsal root ganglion Transgeni GCaMP	Transgenic YFP with Thy1 promoter, transgenic GCaMP6 with Thy1 promoter	17 neurons with YFP, ~50 neurons with GCaMP6	Chen and others (2019a)
Dorsal root ganglion Transgeni	Transgenic GCaMP6 with Cre-inducible promoter	~70 neurons	Chen and others (2019b)
Trigeminal ganglion Transgeni GCaMP	Transgenic GCaMP3 with Pirt promoter; Transgenic GCaMP6 with Cre-inducible promoter	~1050–1170 neurons	Leijon and others (2019)
Dorsal root ganglion Intraplantar-inj	Intraplantar-injected AAV-encoded GCaMP6 in TrpVI ⁺ cells	~140 neurons/ animal	Wang and others (2018)
Dorsal root ganglion GCaMP6	GCaMP6 via AAV with Cre-inducible promoter	200-300 neurons	Chisholm and others (2018)
Trigeminal ganglion, Transgeni dorsal root ganglion	Transgenic GCaMP6 with Cre-inducible promoter	>2000 neurons in trigeminal ganglion. Total neurons imaged in dorsal root ganglion not specified	Ghitani and others (2017)
Trigeminal ganglion GCaMP5/	GCaMP5A with Cre-inducible promoter	>2000 neurons	Yarmolinsky and others (2016)
Dorsal root ganglion Transgeni GCaMP	Transgenic GCaMP3 with Pirt promoter; transgenic GCaMP6 with Cre-inducible promoter	100- 350 neurons	Emery and others (2016)
Dorsal root ganglion Transgeni	Transgenic GCaMP3 with Pirt promoter	>1600 neurons	Kim and others (2016)
	Transgenic GCaMP3 with Pirt promoter	Total neurons visualized per animal not described	Wu and others (2015)
Geniculate ganglion Transgeni	Transgenic GCaMP3 with Thy I promoter	25–30 neurons evoked by taste— total neurons visualized not described	Baretto and others (2015)

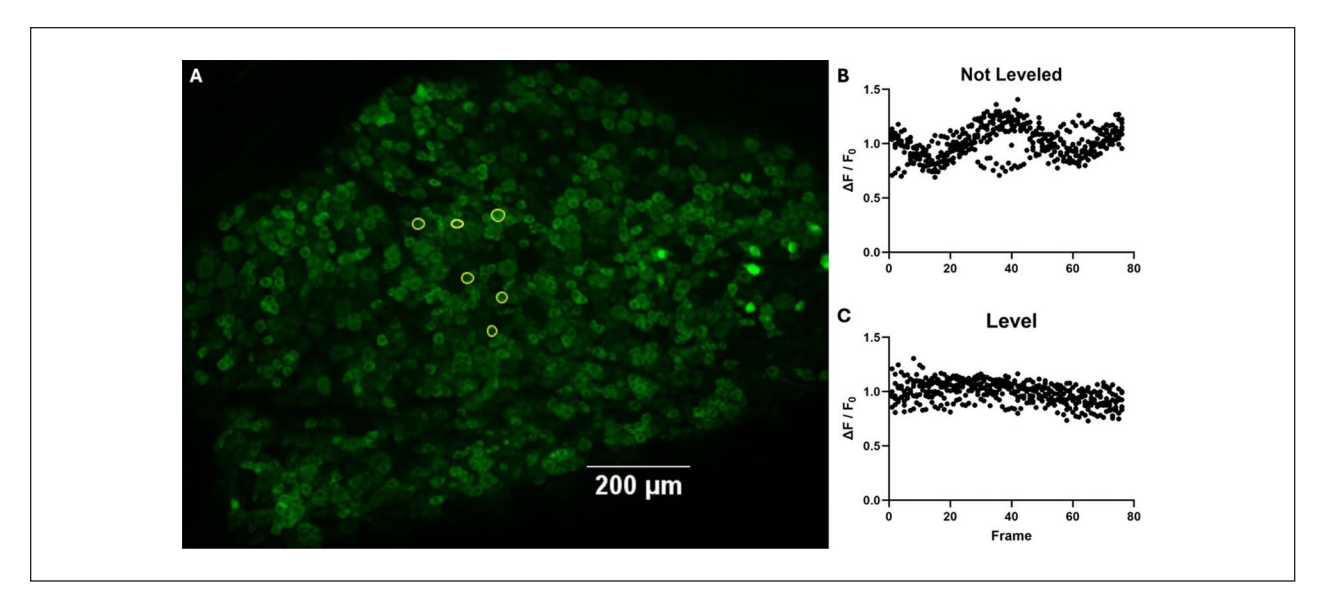


Figure 1. Proper leveling and adjusting are important for dorsal root ganglion imaging. Dealing with motion artifacts by adjusting the position of the spine using spinal clamps to level a lumbar 5 dorsal root ganglion imaged using confocal scanning laser microscopy in a Pirt-GCaMP3 mouse. (A) A sum intensity projection of a confocal scanning laser microscope of a lumbar 5 dorsal root ganglion without stimulus. Spinal clamps immediately rostral and caudal to the ganglion hold it in place. Six neurons are selected. (B) A graph of fluorescent intensity of the six selected neurons normalized to F_0 of median intensity scanning 76 frames over 10 minutes. The six neurons are graphed at each time point. (C) The same six neurons graphed at each time point after the dorsal root ganglion has been leveled by adjusting spinal clamps.

Dealing with Motion Artifacts

A major recurring technical challenge was stabilizing the spine so that heartbeat and breathing motion did not interfere with image resolution. Brain imaging uses the skull as a stable platform to hold the head in place, so there is no difficulty in maintaining cells in the focal plane over time. However, spine imaging has difficulty maintaining cells in the focal plane over time because the spine is flexible and close to the moving internal organs. Another technical challenge is determining baseline fluorescence and spontaneous activity of neurons. A stable platform allows researchers to take multiple images of cells to determine baseline fluorescence and spontaneous activity, but the spinal cord can easily move, making it difficult to determine these. When using two-photon microscopy near myelinated tracts, motion artifacts are exacerbated by myelin's property of scattering light (Wang and others 2005), reducing the overall signal. Methods to address this motion-induced technical challenge include custom spinal clamps placed immediately anterior and distal to the spinal resection (Davalos and others 2008; Johannssen and Helmchen 2010) (Fig. 1), chamber or microprism implants for anesthetized (Farrar and others 2012) and freely moving animals (Sekiguchi and others 2016; Shekhtmeyster and others 2023a), and algorithmic methods (Ahanonu and others 2024).

Imaging Primary Sensory Neurons

Axonal fibers of the primary sensory ganglia innervate the skin, underlying tissues such as muscle, and spinal cord, and initiate somatosensory signals in the nervous system. The dorsal root ganglion (DRG) consists of 10,000–15,000 primary sensory neurons (Schmalbruch 1987; Sørensen and others 2003). Its dorsal location on the lateral aspect of the spine makes it particularly easy to image in vivo. The number of cells imaged in the DRG tends to be much higher than in the dorsal horn (DH). The trigeminal, geniculate, and nodose peripheral ganglia have also been successfully imaged in vivo.

Exposure Surgery of Dorsal Root Ganglia and Trigeminal Ganglia

Intact, entire primary sensory ganglia can be surgically exposed and imaged in vivo (Anderson and others 2018; Chen and others 2019b; Chisholm and others 2018; Emery and others 2016; Ghitani and others 2017; Hu 2019; Huerta and others 2023; Iseppon and others 2023; Kim and others 2016; Leijon and others 2019; Yarmolinsky and others 2016; Zheng and others 2022). This has the powerful advantage of allowing simultaneous observation of thousands of neurons, which has led to the discovery of physiologically relevant phenomena.

Early experiments imaging the DRG in vivo in anesthetized animals found that, surprisingly, over 1600 primary sensory neurons could be imaged simultaneously (Chisholm and others 2018; Emery and others 2016; Ishida and others 2021; Kim and others 2016; Shannonhouse and others 2022; Zheng and others 2022). These experiments led to the discovery of the physiologically relevant phenomenon of coupled activation of adjacent primary sensory neurons in mice following nerve injury or inflammatory insult (Kim and others 2016). Similarly, sympathetic innervation of the DRG after nerve injury, but not following inflammatory insult, was detected via clusters of neurons that activated together (Zheng and others 2022). Other experiments using this system found that more than 85% of primary sensory nociceptive neurons were monomodal when comparing noxious heat, cold, and mechanical stimuli at the population level. Of note, a much higher proportion of primary sensory neurons responded to both cold and heat when cultured in vitro than in vivo (Emery and others 2016). Spontaneous neuronal activity in the L4 DRG following transection of the L5 nerve in rats was robustly increased, complementing similar but smaller-scale electrophysiological data from rats (Chen and others 2019b). Satellite glial cell Ca²⁺ transients can also be monitored (Jager and others 2024).

Similar imaging experiments were performed in the trigeminal ganglion of anesthetized animals following exposure surgery. When all primary sensory neurons and specific populations of TRPV1, TRPA1, and TRPM8 neurons were imaged as a population to measure calcium activity in response to temperature changes in the mouth, 90% of the temperature-sensitive neurons responded to either heat or cold, but not both. Cold-sensitive neurons had three distinct subpopulations, corresponding to adaptation to innocuous or noxious cold (Yarmolinsky and others 2016). Population-level analysis allowed the identification of subpopulations sensitive to temperature and drugs (capsaicin, AITC, and menthol) at concentrations found in food. The response of neuronal populations to temperatures ranging from 5°C to 52°C before and after drug treatment allowed the monitoring of threshold changes in thousands of individual neurons (Leijon and others 2019). Combination of trigeminal ganglion (TG) and DRG imaging revealed that CGRP neurons were thermoreceptors, a novel class of high-threshold mechanoreceptors (HTMRs), or both, but did not respond to gentle touch. Using rapidly adapting GCaMP6, the researchers were able to detect individual action potentials, measure conduction velocity between stimuli and calcium influx, and demonstrate overlapping receptive fields of individual neurons while imaging whole TG or DRG in vivo (Chisholm and others 2018).

Importantly, these imaging methods allowed population-level analysis of primary sensory neuron activity that would otherwise be difficult or impossible using electrophysiological, histological, or other methods. Specific neuron subtypes can be visualized with genetic fluorescent labeling alongside calcium indicators (Kim and others 2016) (Fig. 2). This allowed for population-level studies of changes in coding, multimodality, and neuronal activity patterns under conditions of injury. However, as with spinal cord imaging, these experiments involve terminal surgery, preclude repeated imaging over several hours, and require anesthesia during imaging. They mostly look at neurons on the surface of the ganglia. Neuronal activity patterns have often been correlated with behavior (Alshangiti and others 2024; Chisholm and others 2018; Chivers and others 2024; Emery and others 2016; Ghitani and others 2017; Iseppon and others 2023; Ishida and others 2021; Kim and others 2016; Son and others 2024a, 2024b, 2024c; Yarmolinsky and others 2016; Zheng and others 2022), indicating that calcium imaging is a valid surrogate for neuronal activity in awake mice despite these limitations.

Imaging of Primary Sensory Ganglia in Awake, Behaving Animals and Repetitive Imaging

Imaging DRG neurons in awake, behaving mice is technically challenging due to the flexible nature of the spine, the small size of the DRG, and the fact that the spinal resection method used to create the spinal window removes bone that holds the DRG in place. A group of researchers successfully imaged the DRG by creating a spinal fusion surgical model that minimized spinal motion and secured the imaging chamber in place relative to the microscope objective. Using this method, they were able to repeatedly image the DRG in awake mice for five weeks. Anesthetized mice showed significantly less spontaneous DRG activity than awake mice. The researchers were able to correlate DRG activity over time with phasic pain behavior after formalin injection (Chen and others 2019a). However, the number of neurons that could be imaged in this manner was much smaller than in open surgery, hindering robust population-level analysis of neuronal patterns and detection of rare but physiologically important activity patterns. Although in vivo DRG imaging is technically challenging, in vivo trigeminal ganglion imaging is a promising approach because the skull provides a naturally stable platform for mounting lenses in a manner similar to in vivo brain imaging.

Imaging of Geniculate and Nodose Ganglia

In addition to DRG imaging, a genetically encoded calcium indicators (GECIs) have been successfully used to analyze population-level activity in the geniculate ganglion (GG) in response to gustatory stimuli. A

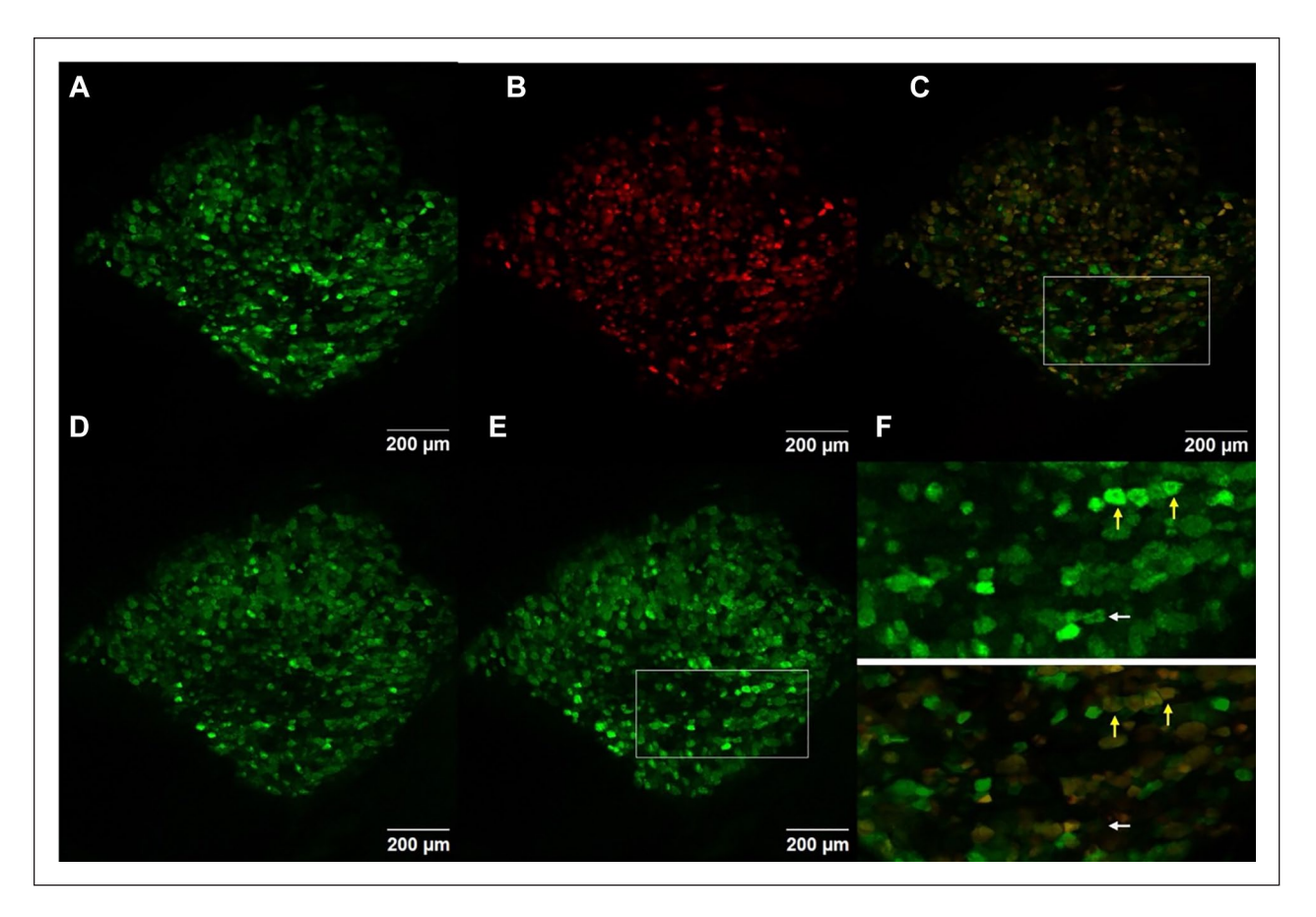


Figure 2. Labeling of specific neurons with Td-Tomato in a lumbar 5 dorsal root ganglion of a Pirt-GCaMP3/NPY2r-Cre td-Tomato mouse imaged using confocal scanning laser microscopy. (A) A high-resolution image of the green (GCaMP3) channel. (B) A high-resolution image of the red (Tomato) channel. (C) Merge of GCaMP3 and Tomato labels. (D) A maximum-intensity projection of GCaMP3 in the baseline period before stimulus. (E) A maximum-intensity projection of GCaMP3 during a 300-gram press on the ipsilateral hind paw. (F) Insets of boxes in panels C and E showing neurons activating during a 300-gram press that are colabeled with Tomato (yellow arrows) or not labeled with Tomato (white arrow).

pioneering study of gustatory stimuli in the GG using implanted lenses found that most neurons responded to only one of five gustatory stimuli (Barretto and others 2015). In contrast, another study using exposure surgery found that relatively few neurons responded to multiple stimuli at low intensities, but about half responded to multiple gustatory stimuli at high intensities (Wu and others 2015). One study was able to selectively label and identify patterns of geniculate neurons in the geniculate ganglion (Asencor and others 2022). Another study investigated TrpV1 and TrpA1 agonists and glutamate applied to the vagus nerve in the nodose ganglion (Huerta and others 2023). Although these studies were able to analyze patterns, they were unable to correlate the observed neural activity with behavior. However, studies using calcium imaging were able to correlate the observed neural activity in the nodose ganglion and geniculate ganglia with a variety of physiological effects (Fowler and others 2022).

High Temporal Resolution Calcium Imaging

A drawback of calcium indicators is that they do not directly image action potentials. Temporal resolution is low, especially when imaging large areas with scanning microscopy, where each scan can take several seconds. However, using a fast version of the GCaMP6 calcium indicator, GCaMP6f, one set of researchers was able to image at frame rates of less than one second and resolve single action potentials evoked in the sciatic nerve. Interestingly, using this method, the researchers found that most neurons showed multimodal responses (to both thermal and mechanical pinch), in contrast to previously published in vivo imaging studies of DRGs (Chisholm and others 2018). These experiments demonstrate that sensitive GECIs can be used to monitor action potentialdriven calcium dynamics at the population level. Furthermore, they suggest that high temporal resolution

analysis of neuronal action potential-mediated calcium dynamics reveals significantly different response patterns than low temporal resolution methods. It should be noted that only one publication exists with this kind of analysis, that individual action potential-mediated calcium transients could only be observed at low firing frequency, and that action potential-mediated calcium influx, not action potentials themselves, were observed.

Imaging Ca²⁺ Transients: Selection and Quantification of Responses

Different methods of calcium imaging analysis can lead to different conclusions. In many fields, including but not limited to neuroimaging (Botvinik-Nezer and others 2020), the same data have been analyzed using different methods in different laboratories or within the same laboratory, resulting in different conclusions. Therefore, it is useful to review different analytical approaches to identify which neurons to include or exclude in the analysis and how to quantify Ca²⁺ transients.

Identification of Ca⁺² Transients

The task of identifying neurons that respond to stimuli or are spontaneously activated can be accomplished using vision, software, or a combination of the two (Table 3). The first method, using vision, can be accomplished by identifying all neurons with Ca²⁺ markers or selectively analyzing neurons that exhibit Ca2+ transients. The advantage of visually observing all cells is that it allows for the analysis of the proportion of cells that responded (e.g., the proportion of cells with different diameters). However, this approach is usually used to observe relatively small numbers of neurons or glial cells, ranging from fewer than 20 to about 400 cells (Barretto and others 2015; Chen and others 2019a; Nishida and others 2014; Ran and others 2016; Sekiguchi and others 2016), although it can be used to characterize thousands of neurons (Son and others 2024a). The disadvantage of this analysis is that it is labor-intensive. Another disadvantage is that it requires long exposures or high laser intensity scans to identify dim cells, consequently resulting in the risk of photobleaching or phototoxicity. The second method is to use software or vision and software to find visually responsive cells (Chisholm and others 2018; Johannssen and Helmchen 2010; Chen and others 2019; Ghitani and others 2017; Yarmolinksy and other 2016; Kim and others 2016; Wu and others 2015; Barretto and others 2015; Kerschensteinner and others 2005; Dray and others 2009; Sørensen and others 2003) (Ingram and others 2024) (Table 3). Analyzing only responsive cells minimizes the need for high-intensity laser scanning or long exposure times, since cells can be identified at their

brightest fluorescence intensity. This approach is therefore less likely to cause phototoxicity and is less laborintensive than analyzing all cells. However, this analysis must be based on the total number of activated cells, not the percentage of activated cells, and therefore may require imaging a large number of animals to obtain clear results, since the size of the area that can be imaged after surgery varies. Researchers must also be careful not to overlook responsive cells, especially dim cells, which can skew the results. Multimodality can be analyzed by selecting only responsive neurons and performing a ratiometric analysis on these (e.g., examining the proportion of neurons that respond to warm temperatures that also react to cold temperatures) (Chisholm and others 2018; Emery and others 2016; Leijon and others 2019). Most published papers rely in whole or in part on humans to identify Ca²⁺ transients, although some recent papers have been able to rely on software entirely (Table 3).

Inclusion and exclusion criteria for responding neurons vary widely (Table 3). Almost all published methods for analyzing responses are based on comparison to baseline fluorescence F₀, with inclusion and exclusion based on the amplitude and/or slope of the curve. The duration of the transient can be used as an inclusion criterion. However, scanning microscopy can take several seconds to scan the imaged region. Consequently, if two neurons are activated for the same duration, one may appear in one scan and the other in two consecutive scans, depending on their location in the imaged region. Scanning microscopy images represent samples taken several seconds apart and cannot be considered a true indicator of transient duration. Scans that take several seconds each confound the analysis of the area under the curve. For such an analysis to be meaningful, a large number of transients should be imaged, or the researcher should accept that the duration cutoff represents the minimum number of neurons activated during the duration, not the total

Distinguishing between genuine stimulus responses and spontaneous transient responses can be problematic, especially when there are few neurons responding to a stimulus or when there is a lot of spontaneous activity (e.g., experimental lesion models). The baseline period for imaging the spinal cord and enteric ganglia may be too short to identify spontaneously active neurons. Stimuli may also inadvertently activate proprioceptors (or mechanoreceptors when studying proprioception) by inducing movement of the stimulated area. One way to address this problem is to conduct multiple trials (Ran and others 2016; Wu and others 2015). However, this approach runs the risk of desensitization. Researchers can also compare stimulus responses to known anatomical structures, such as neuron diameter (Ishida and others 2021; Kim and others 2016; Shannonhouse and others

Microscopy Method	Identification Method, Inclusion/Exclusion Criteria for Ca^{2+} Transients	Reference
Confocal microscope, two-	Ca ²⁺ transients identified by software trained on manually scored neurons and quality controlled by not detecting transients after Ca ²⁺ transients were blocked with anesthetic.	Ingram and others (2024)
Confocal miniscope	${\sf Ca}^{2^+}$ transients identified by software. Transients included by $\Delta {\sf F}/{\sf F}_0 > {\sf F}_0 + (3 \times \sigma {\sf F}_0)$. ${\sf Ca}^{2^+}$ transients excluded if any peaks during the baseline period had an amplitude >50% of the maximum amplitude during the stimulus period.	Huerta and others (2023)
Confocal scanning	${\sf Ca}^{2^+}$ transients identified visually and quantified using $\Delta F/{\sf F_0}$. ${\sf F_0}$ determined by average of 20 s preceding stimulus. Transients included if derivative of $\Delta F/{\sf F_0} >$ (mean derivative ${\sf F_0}+(3 imes\sigma)$ derivative of ${\sf F_0}$).	Iseppon and others (2023)
Confocal scanning	${\sf Ca}^{2^+}$ transients identified visually and quantified using $\Delta F/F_0$. F_0 determined by average of first two to six frames of each experiment. Transients included if $\Delta F/F_0 > 0.2$.	Shannonhouse and others (2022)
Two-photon microscopy	${\sf Ca}^{2^+}$ transients quantified using $\Delta F/F_0$. Criteria for finding and including neurons and determining F_0 not defined.	Zhang and others (2022)
Confocal scanning; fluorescence microscopy	${\sf Ca}^{2^+}$ transients identified visually and quantified using $\Delta F/F_0$. F_0 determined by average of first two to six frames of each experiment. Transients included by $\Delta F/F_n > 0.2$.	Zheng and others (2022)
Confocal scanning	${\sf Ca}^{2^+}$ transients identified visually and quantified using $\Delta F/F_0$. \vec{F}_0 determined by average of first two to six frames of each experiment. Transients included by $\Delta F/F_n > 0.2$	Ishida and others (2021)
Two-photon	All neurons identified. F_0 was 2 s of the lowest fluorescence. Transients included by $\Delta F/F_0 > F_0 + (3 \times \sigma F_0)$.	Chen and others (2019a)
Confocal scanning	Ca^{2+} transients identified visually and included if $\Delta F/F_0 > 0.2$. F_0 determined by average fluorescence intensity of the first two time points.	Chen and others (2019b)
Confocal scanning	${\sf Ca}^{2^+}$ transients identified visually and included if $\Delta F/{\sf F}_0>{\sf F}_0+(5 imes\sigma{\sf F}_0).$ ${\sf F}_0$ determined by published MATLAB code.	Leijon and others (2019)
Confocal scanning, two-photon scanning	${\sf Ca}^{2^+}$ transients identified visually and included if $\Delta {\sf F/F}_0>1.7+(4 imes\sigma{\sf F}_0).$ ${\sf F}_0$ determined by fluorescence intensity of a baseline period.	Chisholm and others (2018)
Two-photon scanning	${\sf Ca}^{2^+}$ transients identified visually and quantified using $\Delta F/F_0$. F_0 determined by average of first 30 s of each experiment. Transients included if $\Delta F/F_0 > 0.3$.	Yoshihara and others (2018)
Epifluorescence halogen lamp using a standard green excitation/ emission filter	Ca^{2+} transients identified visually. Background of a ring immediately around the neuron was subtracted. Background was the average of five lowest frames of the experiment. Transients included if $\Delta F/F_0 > 0.2$.	Ghitani and others (2017)

Table 3. (continued)		
Microscopy Method	Identification Method, Inclusion/Exclusion Criteria for Ca^{2^+} Transients	Reference
Confocal scanning	Method of identification not described. Fluorescence at each time point was normalized from 0 to I based on minimum and maximum fluorescence. Responding neurons included if the maximum derivative of trace was $>4 \times \sigma$ of the derivative of previous five time points.	Emery and others (2016)
Excitation/filter not specified. 5-Hz single field of view at $4 imes$ to $10 imes$ magnification	${\sf Ca}^{2+}$ transients identified by software and visually confirmed. Transients included if F $>$ 7 $ imes$ median deviation of background. Background defined as neighborhood fluorescence two-cell radii around the cell (excluding other responding neurons). Neurons excluded if another nearby neuron contaminated the signal.	Yarmolinsky and others (2016)
Confocal scanning	Ca^{2+} transients identified visually and quantified using $\Delta F/F_0$. F_0 determined by average of first two to six frames of each experiment.	Kim and others (2016)
Two-photon scanning	Neurons identified using custom MATLAB software and corrected manually. Ca ²⁺ transients included if $\Delta F/F_0 > 0.05 + (5 \times \sigma F_0)$ across multiple trials. F_0 determined by average of 9 s before stimulus.	Ran and others (2016)
One-photon GRIN probe; two-photon scanning	Neurons and glia identified using published MATLAB software or visually identified. MATLAB identified cells were included based on $\Delta F/F_0 > 2 \times \sigma \ F_0$ and visually identified ones included if $\Delta F/F_0 > 0.5$. F, method of determination not specified.	Sekiguchi and others (2016)
Confocal scanning	$Ca^{2+}_{}$ transients identified visually and quantified using peak value of $\Delta F/F_0$. F_0 determined by published MATLAB software. Ca^{2+} transients if peak $\Delta F/F_0 > 2 imes \sigma$ F_n across two stimulus replicates.	Wu and others (2015)
Two-photon GRIN probe, single focal plane	Responding neurons identified both by computer using statistical deviation from baseline during stimulus period and by visual scoring. Traces generated by △F/F. F is median fluorescence. Transients included if deviation from baseline z-score compared to median absolute deviation was >2 for at least 650 ms. Modality categories of <1% of identified neuron population were excluded.	Barretto and others (2015)
Two-photon scanning Custom built two-photon		Nishida and others (2014) Johannsson and Helmchen (2010)

 σ F = standard deviation of fluorescence intensity.

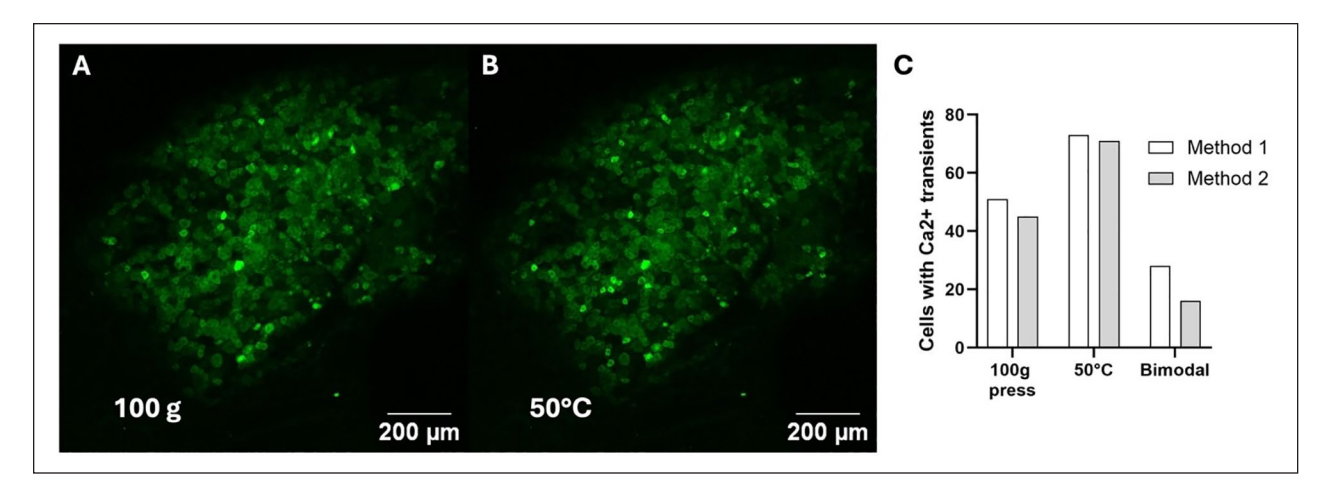


Figure 3. Different methods of inclusion and exclusion of neurons give different results. (A) A maximum-intensity projection of a lumbar 5 dorsal root ganglion in a Pirt-GCaMP3 mouse undergoing a 100-gram press on the ipsilateral hind paw. (B) A maximum-intensity projection of a lumbar 5 dorsal root ganglion in a Pirt-GCaMP3 mouse undergoing ipsilateral hind paw immersion in 50°C water. (C) A graph of the number of producing Ca²⁺ transients during a 100-gram press, 50°C water immersion, and both (bimodal) using the inclusion/exclusion criteria from Shannonhouse and others (2022) (Method I, white bar) and Emery and others (2016) (Method 2, gray bar).

2022) or location (Kohro and others 2020; Shekhtmeyster and others 2023a), to determine if the results are consistent with known properties of the neurons. However, these approaches cannot exclude individual neurons for spontaneous activity and risk overlooking changes in coding that occur in experimental models. Finally, researchers can image enough animals to statistically overwhelm the noise of spontaneous activity. Furthermore, if it is important to distinguish signals originating in the skin rather than underlying tissues such as muscle, methods such as fluorescent tracers injected into the site of interest will be useful.

Baseline Fluorescence

A key issue in calcium imaging analysis is how to establish F₀. The skull can provide a stable platform for fixing the objective at a fixed distance from the brain or TG. This allows for establishing baseline fluorescence and analyzing for long periods of time to determine whether cells are spontaneously active. However, the spinal cord and ganglia are much more difficult to fix in place, so baseline acquisition periods can be very short. For responses to stimulation, F₀ is often the average of the prestimulus period or number of frames, or a defined baseline period (Chen and others 2019b; Chisholm and others 2018; Emery and others 2016; Ghitani and others 2017; Ishida and others 2021; Johannssen and Helmchen 2010; Kim and others 2016; Nishida and others 2014; Ran and others 2016; Sekiguchi and others 2016; Shannonhouse and others 2022; Wu and others 2015). It is important to note that signals from nearby neurons can interfere with the analysis, making it difficult to tell if a faint neuron is activated and making it impossible to accurately measure $\Delta F/F_0$. The difference in fluorescence intensity between baseline fluorescence and fluorescence upon cytosolic Ca²+ influx can vary greatly among fluorophores. For example, GCaMP3 and GCaMP6f evoked in cultured neurons show up to a ninefold difference in $\Delta F/F_0$, suggesting that $\Delta F/F_0$ and exclusion/inclusion criteria are not always comparable across papers.

Fluorophore Properties

Differences in fluorophores and inclusion/exclusion criteria may be the cause of the different results. Researchers have found that the number of neurons activated differs when using different fluorophores in the dorsal root ganglion (Emery and others 2016; Kim and others 2016). In particular, the ratio of mechanical and thermal modalities differed significantly in the papers that studied DRG neuron modalities. One potential explanation is that one study included neurons based on the ratio of the derivative of the stimulus $\Delta F/F_0$ to the standard deviation of the baseline derivatives of $\Delta F/F_0$ (Emery and others 2016), while another study included neurons based on the value of $\Delta F/F_0$ (Chisholm and others 2018). A neuron could appear to be monomodal under one set of inclusion/exclusion criteria and bimodal under different criteria (Fig. 3).

When choosing a fluorophore, considerations include whether the researcher needs to image inactive neurons, the importance of detecting dim neurons, the importance of cell type specificity for the study, and whether the microscope can sample the fluorophore at a sufficient rate

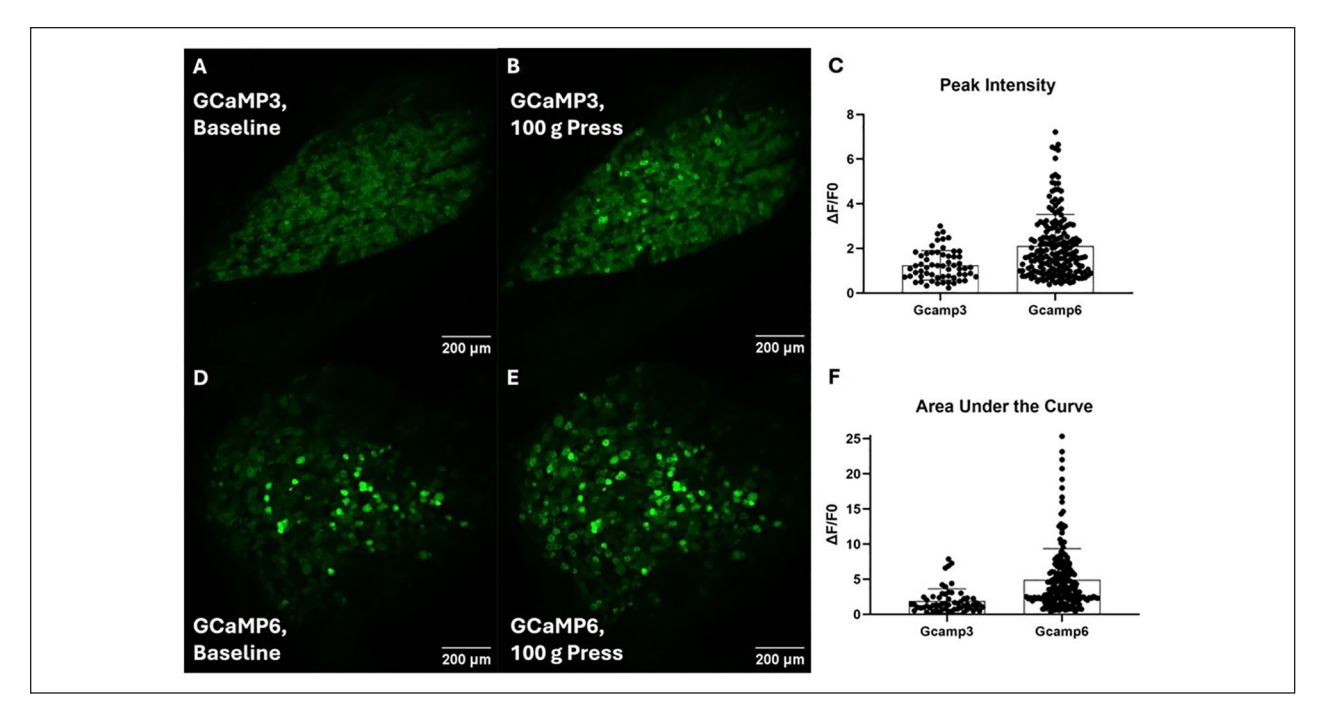


Figure 4. Choice of fluorophore and effect on number and intensity of Ca^{2+} transients detected and the ability to clearly see inactive neurons. (A) A maximum-intensity projection of a lumbar 5 dorsal root ganglion in a Pirt-GCaMP3 mouse using confocal laser scanning microscopy in the absence of stimulus. (B) The same ganglion as panel A during a 100-gram press on the ipsilateral hind paw. (C) A graph of maximum peak $\Delta F/F_0$ intensity of all individual Ca^{2+} transients during a 100-gram press on the ipsilateral hind paw in a Pirt-GCaMP3 mouse and a Pirt-Cre GCaMP6s mouse. (D) A maximum-intensity projection of a lumbar 5 dorsal root ganglion in a Pirt-Cre GCaMP6 mouse using confocal laser scanning microscopy in the absence of stimulus. (E) The same ganglion as panel during a 100-gram press on the ipsilateral hindpaw. (F) A graph of the area under the curve of $\Delta F/F_0$ intensity of all individual Ca^{2+} transients during a 100-gram press on the ipsilateral hindpaw in a Pirt-GCaMP3 mouse and a Pirt-Cre GCaMP6s mouse.

for the study. Baseline brightness becomes important if the researcher chooses to look at all neurons in a region rather than just active neurons. Although the GCaMP6 isoform is brighter than other GECIs used to image spinal cord or sensory ganglia, it has low baseline fluorescence at normal physiological Ca2+ concentrations (Chen and others 2013), and in the experience of these authors, it is difficult to see inactive neurons expressing GCaMP6 in peripheral ganglia (Fig. 4). GCaMP5 has similarly low baseline brightness (Akerboom and others 2012), and GCaMP7 and GCaMP8 are much lower (Ohkura and others 2012). GCaMP3 has a higher baseline brightness (Akerboom and others 2012; Tian and others 2009), making it easier to identify inactive neurons. If the investigator plans to analyze only active neurons, the microscope should be able to detect the maximum brightness during a Ca²⁺ transient (for positively modulated indicators) or the baseline (for negatively modulated indicators). Ratiometric dyes emit alternate wavelengths with relative intensities depending on Ca²⁺ concentrations. Microscopes that are not designed to rapidly switch back and forth or to excite and detect both wavelengths simultaneously have very limited ability to image Ca²⁺ transients in vivo using ratiometric dyes (Bootman and others 2013) or genetically encoded FRET Ca²⁺ indicators.

Future Directions in Primary Sensory Neuron and Spinal Cord Imaging

Imaging with calcium-sensitive fluorophores has been a powerful method for studying neurons and other cell types in vivo at the population level and for repeatedly imaging the same cells under a variety of conditions. Future directions in this research include combining calcium imaging approaches with optogenetics, imaging in awake mice, and combining imaging with other fluorescent biosensors, such as voltage-sensor imaging, and other second messengers, such as cAMP sensor imaging.

Optogenetics and Red Fluorescent GECIs

Optogenetics is a powerful way to depolarize or hyperpolarize cells via light-sensitive ion channels such

as channelrhodopsin (Nagel and others 2003) and the light-activated chloride pump halorhodopsin (Zhao and others 2008). Unfortunately, the wavelengths of light required to excite green fluorescent GECIs or green fluorescent calcium-sensitive fluorescent dyes also activate many optogenetic channels, such as channelrhodopsin and halorhodopsin. A solution could be red fluorescent calcium indicators that are designed to be unaffected by the blue light used in optogenetics (Dana and others 2016; Hussein and Berlin 2020) or red-shifted channelrhodopsins (Lin and others 2013; Turrini and others 2024). By controlling genetically encoded optogenetic proteins under cell type-specific Cre recombinase, it should be possible to reversibly activate and deactivate specific cell types and analyze their effects on calcium dynamics and activity elsewhere in the neural network. This has been demonstrated in albino zebrafish larvae using acoustooptic deflectors and light sheet microscopy (Turrini and others 2024), although this technology may not be currently suitable for mammalian use.

Genetically Encoded Voltage Indicators for Ultra-Fast Imaging of Action Potentials

GECIs indirectly measure action potentials. Cytosolic calcium monitoring has been used to study efflux from the endoplasmic reticulum, mitochondria, or other types of cell surface receptors (Akerboom and others 2012; Chen and others 2013; Rieder and others 2022; Tian and others 2009). In vitro imaging using GECIs suggests that individual action potential-driven calcium influx can be directly imaged only at relatively low neuronal firing frequencies (Chisholm and others 2018; Hartung and Gold 2020). To directly study action potentials in large populations of neurons, other tools are needed. Voltagesensitive dyes and genetically encoded voltage indicators (GEVIs) may provide important alternatives for imaging action potentials in vivo. Voltage-sensitive dyes have been used to image brain neurons in vivo (Dalphin and others 2020; Kuhn and others 2008; Roome and Kuhn 2018; Roome and Kuhn 2020). GEVIs have been used to image cortical neurons in anesthetized and awake mice, and direct comparison of patch-clamp recordings with fluorescence has demonstrated that GEVIs can be used to directly measure action potentials in vivo (Villette and others 2019). Combining GEVIs with red fluorescent GECIs allows for simultaneous analysis of total cytosolic calcium levels and voltage changes. This approach opens up the exciting possibility of distinguishing between the effects of neuronal firing and the overall physiological state of neurons and their signaling pathways and outcomes.

Other Fluorescent Indicators

In addition to GEVIs, other fluorescent biosensors for intracellular signaling, second messengers, and cell activity markers could potentially be used for in vivo imaging. These sensors can be coupled to calcium or voltage indicators, allowing changes in calcium or voltage to be correlated with cell signaling or cell activity markers. A variety of fluorescent sensors exist for various polyphosphoinositides (PPIns) that can be used to study PPIn signaling and intracellular localization (Hammond and Balla 2015). Fluorescent sensors have also been tested for a variety of other cell signaling and metabolic sensors in mammalian cells. These include cAMP (Harada and others 2017) and cGMP (Calamera and others 2019), ATP/ ADP and ATP/AMP ratios (Crocker and others 2020), lactate/pyruvate ratios (Galaz and others 2020), poly-ADP-ribose (Serebrovskaya and others 2020), and extracellular ATP (Kitajima and others 2020). Many more fluorescent indicators of cell signaling and metabolism have been developed and are continuing to be developed. GRAB (GPCR-activation based) sensors are a general design that exploits conformational changes in the intracellular loop between transmembrane helices 5 and 6 of G protein-coupled receptors, which has enabled the design of a wide range of fluorescent indicators with diverse excitation/emission spectra and sensitivity to a variety of extracellular ligands (Dong and others 2022; Dong and others 2023; Feng and others 2019; Jing and others 2020; Peng and others 2020; Qian and others 2023; Sun and others 2020; Wan and others 2021; Wu and others 2023; Zeng and others 2023). A major advantage of fluorescent sensors is that many standard analyses of the signal require tissue destruction, whereas imaging with fluorescent sensors allows real-time correlation with a resolution of two seconds or even subseconds. The variety of signals and analysis speeds means that fluorescent imaging has the potential to revolutionize the analysis of cell signaling in neurons in vivo. The combination of different excitation and emission wavelengths for GECIs and other sensors will be important for such studies, as they require simultaneous monitoring of calcium and other types of molecules.

Anesthesia and Repetitive Longitudinal Imaging

The choice of whether to allow imaging with or without anesthesia is important and can have a major impact on the cellular activity and pattern generation that can be achieved in the types of experiments that can be performed in vivo. The anesthetics required for exposure surgery can disrupt the activity of certain neurons and

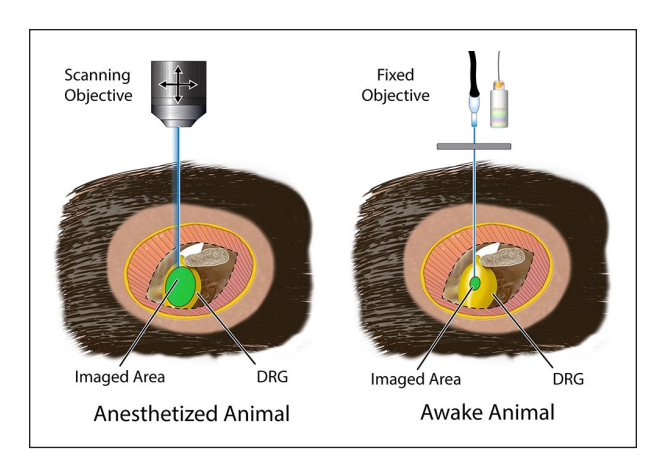


Figure 5. Advantages and disadvantages of imaging anesthetized vs awake animals. (Left) Anesthetized mice can be placed under the scanning objective of a conventional microscope. This allows for wide and deep imaging of tissues such as the dorsal root ganglion (or dorsal horn, trigeminal ganglion, etc.), allowing researchers to monitor calcium activity in hundreds or thousands of cells. However, anesthesia disrupts normal neural activity, and experiments are usually terminal. (Right) Tissues can be imaged repeatedly over several weeks or months in awake and freely moving mice without anesthesia disrupting normal neural activity. However, this requires a special stable platform that is mounted at a fixed distance from the tissue during the imaging session. This significantly limits the number of cells that can be imaged in a single imaging session.

other cell types (Chen and others 2019a; Sekiguchi and others 2016; Shekhtmeyster and others 2023a; Sullivan and Sdrulla 2022). Implanting chambers to image awake animals can avoid this problem but presents unique challenges. Awake animals are mobile and therefore cannot simply be placed under the objective of a conventional microscope, or a scanning confocal or multiphoton microscope, for imaging in vivo. Specialized stable platforms for the imaging window must be mounted to the tissue to be imaged in a fixed position (Fig. 5). As a result, fewer cells can be imaged in awake mice than in anesthetized mice following exposure surgery (tens vs hundreds to thousands). Current techniques therefore have limitations in detecting the broad population-level changes that can be observed and in observing rare but physiologically important patterns of neural activity. However, the observation chamber has the important advantage of allowing repeated imaging of the same cells over multiple sessions spaced several days or weeks apart, allowing experiments such as observing the regeneration and degeneration of individual damaged axons, the neuroplasticity of damaged neurons, or the resulting changes in network activity, and helping to address questions about how anesthesia itself affects neural activity patterns and responses.

Chemigenetic and mNeon Green Indicators

Improving the signal-to-background ratio would improve researchers' ability to detect intracellular calcium changes in neurons where the signal is weak. One approach to this problem is to use chemogenetic sensors or to improve the maximum fluorescence of GECIs (Chai and others 2023). Chemogenetics involves engineering proteins to specifically bind to an injected chemical indicator. This allows researchers to combine the cell-type specificity of a genetic indicator with the sensitivity, brightness, absorbance/emission spectra, and photostability of a chemical indicator (Chai and others 2023; Hoelzel and Zhang 2020; Zhu and others 2023). mNeon Green is a much brighter fluorescent protein than GFP (Shaner and others 2013). Using the GCaMP protein as a model, similar NCaMP proteins have been engineered (Li and others 2023; Subach and others 2020), some of which (NEMO components) have much higher $\Delta F/F_0$ than GCaMP6 (Li and others 2023). However, we were unable to find published examples of chemogenetics or NEMO in spinal cord or peripheral ganglia in vivo.

Conclusions

Imaging calcium activity is one of the most powerful methods for studying neural network activity in the primary somatosensory ganglia and the spinal cord. Exposure surgery can visualize large areas of the spinal cord and entire peripheral ganglia but requires anesthesia. In contrast, implanting an observation chamber allows monitoring of neurons in relatively small areas. Calcium signaling can indirectly monitor action potentials in up to thousands of neurons. New red fluorescent calcium indicators allow researchers to combine the power of optogenetics with calcium signaling. Combining red or green emitting calcium indicators with other types of indicators, such as voltage, metabolic indicators, or cAMP, reduces these confounding factors.

Cytosolic calcium levels can be used to monitor action potentials via calcium influx, ligand binding to voltagegated and ligand-gated channels, and calcium efflux from the endoplasmic reticulum or mitochondria.

A variety of sensors and manipulations can be combined with calcium imaging (Fig. 6). Optogenetics using channelrhodopsin and halorhodopsin are stimulated by blue wavelengths and can be used with red calcium indicators. Depending on the emission wavelength, green or red fluorescent GECIs can be imaged simultaneously with markers of intracellular signaling (e.g., cAMP, cGMP, PPIn) or cell metabolism (e.g., AMP/ATP ratio, lactate/pyruvic acid ratio). A wide variety of GRAB sensors detect extracellular neurotransmitters. Fluorescent indicators allow rapid detection and

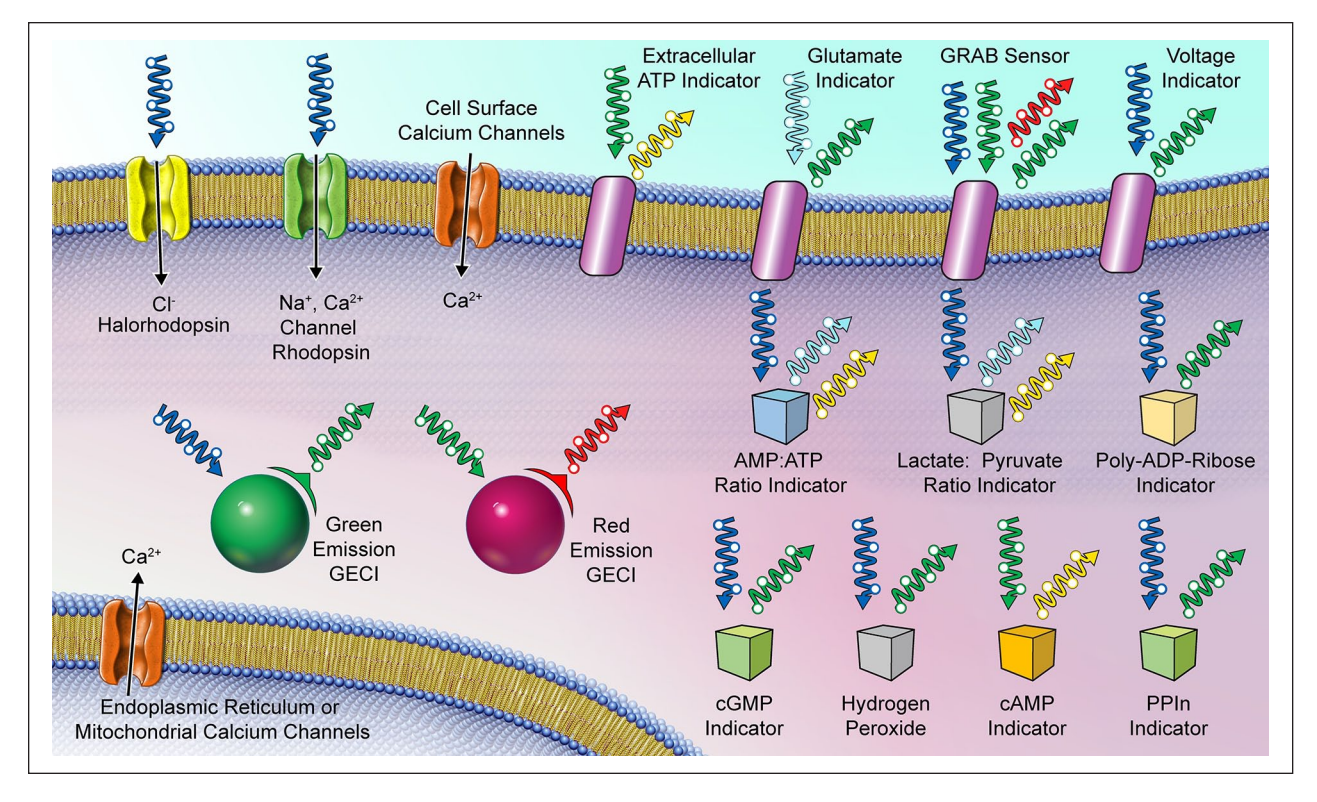


Figure 6. Simultaneous imaging of calcium activity and other cellular activity markers.

analysis of these cell signaling markers during imaging without damaging the tissue under physiological conditions in vivo. Voltage-sensitive dyes or GEVIs can directly detect voltage changes. Combining fluorescent voltage sensors with fluorescent calcium sensors that emit at different wavelengths allows simultaneous monitoring of voltage changes and intracellular calcium dynamics.

Acknowledgments

We thank members of the Kim laboratory for helpful comments and discussion.

Declaration of Conflicting Interests

The author(s) declared no potential conflicts of interest with respect to the research, authorship, and/or publication of this article.

Funding

The author(s) disclosed receipt of the following financial support for the research, authorship, and/or publication of this article: This work was supported by National Institutes of Health Grant (R01DE031477 and R01NS128574 to Y.K.) and a STAR Award from the University of Texas system and NIH T32DE014318 COSTAR award (J.S.).

ORCID iDs

Joon Tae Park https://orcid.org/0000-0003-2396-9108 Yu Shin Kim https://orcid.org/0000-0002-6677-5656

References

Ahanonu B, Crowther A, Kania A, Rosa-Casillas M, Basbaum AI. 2024. Long-term optical imaging of the spinal cord in awake behaving mice. Nat Methods 21(12):2363–75.

Akerboom J, Chen TW, Wardill TJ, Tian L, Marvin JS, Mutlu S, and others. 2012. Optimization of a GCaMP calcium indicator for neural activity imaging. J Neurosci 32(40):13819–40.

Alshanqiti I, Son H, Shannonhouse J, Hu J, Kumari S, Parastooei G, and others. 2024. Posttraumatic hyperalgesia and associated peripheral sensitization after temporomandibular joint injury in mice. Pain 166(7):1597–609.

Anderson M, Zheng Q, Dong X. 2018. Investigation of pain mechanisms by calcium imaging approaches. Neurosci Bull 34(1):194–9.

Asencor AI, Dvoryanchikov G, Makhoul V, Tsoulfas P, Chaudhari N. 2022. Selectively imaging cranial sensory ganglion neurons using AAV-PHP.S. eNeuro 9(3):ENE URO.0373-21.2022.

Barretto RP, Gillis-Smith S, Chandrashekar J, Yarmolinsky DA, Schnitzer MJ, Ryba NJ, and others. 2015. The neural representation of taste quality at the periphery. Nature 517(7534):373–6.

Bootman MD, Rietdorf K, Collins T, Walker S, Sanderson M. 2013. Ca2+-sensitive fluorescent dyes and intracellular Ca2+ imaging. Cold Spring Harb Protoc 2013(2):83–99.

- Botvinik-Nezer R, Holzmeister F, Camerer CF, Dreber A, Huber J, Johannesson M, and others. 2020. Variability in the analysis of a single neuroimaging dataset by many teams. Nature 582(7810):84–88.
- Calamera G, Li D, Ulsund AH, Kim JJ, Neely OC, Moltzau LR, and others. 2019. FRET-based cyclic GMP biosensors measure low cGMP concentrations in cardiomyocytes and neurons. Commun Biol 2:394.
- Chai F, Cheng D, Nasu Y, Terai T, Campbell RE. 2023. Maximizing the performance of protein-based fluorescent biosensors. Biochem Soc Trans 51(4):1585–95.
- Chen C, Zhang J, Sun L, Zhang Y, Gan WB, Tang P, and others. 2019a. Long-term imaging of dorsal root ganglia in awake behaving mice. Nat Commun 10(1):3087.
- Chen T, Taniguchi W, Chen QY, Tozaki-Saitoh H, Song Q, Liu RH, and others. 2018. Top-down descending facilitation of spinal sensory excitatory transmission from the anterior cingulate cortex. Nat Commun 9(1):1886.
- Chen TW, Wardill TJ, Sun Y, Pulver SR, Renninger SL, Baohan A, and others. 2013. Ultrasensitive fluorescent proteins for imaging neuronal activity. Nature 499(7458):295–300.
- Chen Z, Wang T, Fang Y, Luo D, Anderson M, Huang Q, and others. 2019b. Adjacent intact nociceptive neurons drive the acute outburst of pain following peripheral axotomy. Sci Rep 9(1):7651.
- Cheng YT, Lett KM, Schaffer CB. 2019. Surgical preparations, labeling strategies, and optical techniques for cell-resolved, in vivo imaging in the mouse spinal cord. Exp Neurol 318:192–204.
- Chisholm KI, Khovanov N, Lopes DM, La Russa F, McMahon SB. 2018. Large scale in vivo recording of sensory neuron activity with GCaMP6. eNeuro 5(1):ENE URO.0417-17.2018.
- Chivers SB, Andrade MA, Hammack RJ, Shannonhouse J, Gomez R, Zhang Y, and others. 2024. Peripheral macrophages contribute to nociceptor priming in mice with chronic intermittent hypoxia. Sci Signal 17(847):eadn8936.
- Crocker H, Pelosse M, Schlattner U, Berger I. 2020. AMPfret: synthetic nanosensor for cellular energy states. Biochem Soc Trans 48(1):103–11.
- Dalphin N, Dorgans K, Khaskin E, Kuhn B. 2020. Voltage imaging of cortical oscillations in layer 1 with two-photon microscopy. eNeuro 7(3):ENEURO.0274-19.2020.
- Dana H, Mohar B, Sun Y, Narayan S, Gordus A, Hasseman JP, and others. 2016. Sensitive red protein calcium indicators for imaging neural activity. Elife 5:e12727.
- Davalos D, Lee JK, Smith WB, Brinkman B, Ellisman MH, Zheng B, and others. 2008. Stable in vivo imaging of densely populated glia, axons and blood vessels in the mouse spinal cord using two-photon microscopy. J Neurosci Methods 169(1):1–7.
- Dong A, He K, Dudok B, Farrell JS, Guan W, Liput DJ, and others. 2022. A fluorescent sensor for spatiotemporally resolved imaging of endocannabinoid dynamics in vivo. Nat Biotechnol 40(5):787–98.

- Dong H, Li M, Yan Y, Qian T, Lin Y, Ma X, and others. 2023. Genetically encoded sensors for measuring histamine release both in vitro and in vivo. Neuron 111(10):1564–76. e6.
- Dray C, Rougon G, Debarbieux F. 2009. Quantitative analysis by in vivo imaging of the dynamics of vascular and axonal networks in injured mouse spinal cord. Proc Natl Acad Sci U S A 106(23):9459–64.
- Emery EC, Luiz AP, Sikandar S, Magnúsdóttir R, Dong X, Wood JN. 2016. In vivo characterization of distinct modality-specific subsets of somatosensory neurons using GCaMP. Sci Adv 2(11):e1600990.
- Evans TA, Barkauskas DS, Myers JT, Hare EG, You JQ, Ransohoff RM, and others. 2014. High-resolution intravital imaging reveals that blood-derived macrophages but not resident microglia facilitate secondary axonal dieback in traumatic spinal cord injury. Exp Neurol 254:109–20.
- Fadaka AO, Dourson AJ, Hofmann MC, Gupta P, Raut NGR, Jankowski MP. 2025. The intersection of endocrine signaling and neuroimmune communication regulates muscle inflammation-induced nociception in neonatal mice. Brain Behav Immun 125:198–211.
- Farrar MJ, Bernstein IM, Schlafer DH, Cleland TA, Fetcho JR, Schaffer CB. 2012. Chronic in vivo imaging in the mouse spinal cord using an implanted chamber. Nat Methods 9(3):297–302.
- Feng J, Zhang C, Lischinsky JE, Jing M, Zhou J, Wang H, and others. 2019. A genetically encoded fluorescent sensor for rapid and specific in vivo detection of norepinephrine. Neuron 102(4):745–61.e8.
- Fowler BE, Ye J, Humayun S, Lee H, Macpherson LJ. 2022. Regional specialization of the tongue revealed by gustatory ganglion imaging. iScience 25(12):105700.
- Galaz A, Cortés-Molina F, Arce-Molina R, Romero-Gómez I, Mardones GA, Felipe Barros L, and others. 2020. Imaging of the lactate/pyruvate ratio using a genetically encoded förster resonance energy transfer indicator. Anal Chem 92(15):10643–50.
- Ghitani N, Barik A, Szczot M, Thompson JH, Li C, Le Pichon CE, and others. 2017. Specialized mechanosensory nociceptors mediating rapid responses to hair pull. Neuron 95(4):944–54.e4.
- Hammond GR, Balla T. 2015. Polyphosphoinositide binding domains: key to inositol lipid biology. Biochim Biophys Acta 1851(6):746–58.
- Harada K, Ito M, Wang X, Tanaka M, Wongso D, Konno A, and others. 2017. Red fluorescent protein-based cAMP indicator applicable to optogenetics and in vivo imaging. Sci Rep 7(1):7351.
- Hartung JE, Gold MS. 2020. GCaMP as an indirect measure of electrical activity in rat trigeminal ganglion neurons. Cell Calcium 89:102225.
- Helmchen F, Imoto K, Sakmann B. 1996. Ca2+ buffering and action potential-evoked Ca2+ signaling in dendrites of pyramidal neurons. Biophys J 70(2):1069–81.
- Hoelzel CA, Zhang X. 2020. Visualizing and manipulating biological processes by using HaloTag and SNAP-Tag technologies. Chembiochem 21(14):1935–46.

Hu M. 2019. Visualization of trigeminal ganglion neuronal activities in mice. Curr Protoc Cell Biol 83(1):e84.

- Huerta TS, Haider B, Adamovich-Zeitlin R, Chen AC, Chaudhry S, Zanos TP, and others. 2023. Calcium imaging and analysis of the jugular-nodose ganglia enables identification of distinct vagal sensory neuron subsets. J Neural Eng 20(2):10.1088/1741-2552/acbe1e.
- Hussein W, Berlin S. 2020. Red photoactivatable genetic optical-indicators. Front Cell Neurosci 14:113.
- Ikeda H, Stark J, Fischer H, Wagner M, Drdla R, Jäger T, and others. 2006. Synaptic amplifier of inflammatory pain in the spinal dorsal horn. Science 312(5780):1659–62.
- Ingram S, Chisholm KI, Wang F, De Koninck Y, Denk F, Goodwin GL. 2024. Assessing spontaneous sensory neuron activity using in vivo calcium imaging. Pain 165(5):1131–41.
- Iseppon F, Luiz AP, Linley JE, Wood JN. 2023. Pregabalin silences oxaliplatin-activated sensory neurons to relieve cold allodynia. eNeuro 10(2):ENEURO.0395-22.2022.
- Ishida H, Zhang Y, Gomez R, Shannonhouse J, Son H, Banik R, and others. 2021. In vivo calcium imaging visualizes incision-induced primary afferent sensitization and its amelioration by capsaicin pretreatment. J Neurosci 41(41):8494–507.
- Jager SE, Goodwin G, Chisholm KI, Denk F. 2024. In vivo calcium imaging shows that satellite glial cells have increased activity in painful states. Brain Commun 6(2):fcae013.
- Jing M, Li Y, Zeng J, Huang P, Skirzewski M, Kljakic O, and others. 2020. An optimized acetylcholine sensor for monitoring in vivo cholinergic activity. Nat Methods 17(11):1139–46.
- Johannssen HC, Helmchen F. 2010. In vivo Ca2+ imaging of dorsal horn neuronal populations in mouse spinal cord. J Physiol 588(Pt 18):3397–402.
- Johansson RS, Flanagan JR. 2009. Coding and use of tactile signals from the fingertips in object manipulation tasks. Nat Rev Neurosci 10(5):345–59.
- Kawanabe R, Yoshihara K, Hatada I, Tsuda M. 2021. Activation of spinal dorsal horn astrocytes by noxious stimuli involves descending noradrenergic signaling. Mol Brain 14(1):79.
- Kerschensteiner M, Schwab ME, Lichtman JW, Misgeld T. 2005. In vivo imaging of axonal degeneration and regeneration in the injured spinal cord. Nat Med 11(5):572–7.
- Kim YS, Anderson M, Park K, Zheng Q, Agarwal A, Gong C, and others. 2016. Coupled activation of primary sensory neurons contributes to chronic pain. Neuron 91(5):1085– 96.
- Kitajima N, Takikawa K, Sekiya H, Satoh K, Asanuma D, Sakamoto H, and others. 2020. Real-time in vivo imaging of extracellular ATP in the brain with a hybrid-type fluorescent sensor. Elife 9:e57544.
- Kohro Y, Matsuda T, Yoshihara K, Kohno K, Koga K, Katsuragi R, and others. 2020. Spinal astrocytes in superficial laminae gate brainstem descending control of mechanosensory hypersensitivity. Nat Neurosci 23(11):1376–87.
- Kuhn B, Denk W, Bruno RM. 2008. In vivo two-photon voltage-sensitive dye imaging reveals top-down control of cortical layers 1 and 2 during wakefulness. Proc Natl Acad Sci U S A 105(21):7588–93.

- Leijon SCM, Neves AF, Breza JM, Simon SA, Chaudhari N, Roper SD. 2019. Oral thermosensing by murine trigeminal neurons: modulation by capsaicin, menthol and mustard oil. J Physiol 597(7):2045–61.
- Li J, Shang Z, Chen JH, Gu W, Yao L, Yang X, and others. 2023. Engineering of NEMO as calcium indicators with large dynamics and high sensitivity. Nat Methods 20(6):918–24.
- Lin JY, Knutsen PM, Muller A, Kleinfeld D, Tsien RY. 2013. ReaChR: a red-shifted variant of channelrhodopsin enables deep transcranial optogenetic excitation. Nat Neurosci 16(10):1499–508.
- Lorenzana AO, Lee JK, Mui M, Chang A, Zheng B. 2015. A surviving intact branch stabilizes remaining axon architecture after injury as revealed by in vivo imaging in the mouse spinal cord. Neuron 86(4):947–54.
- MacDonald DI, Luiz AP, Iseppon F, Millet Q, Emery EC, Wood JN. 2021. Silent cold-sensing neurons contribute to cold allodynia in neuropathic pain. Brain 144(6):1711–26.
- Nagel G, Szellas T, Huhn W, Kateriya S, Adeishvili N, Berthold P, and others. 2003. Channelrhodopsin-2, a directly lightgated cation-selective membrane channel. Proc Natl Acad Sci U S A 100(24):13940-5.
- Nishida K, Matsumura S, Taniguchi W, Uta D, Furue H, Ito S. 2014. Three-dimensional distribution of sensory stimulation-evoked neuronal activity of spinal dorsal horn neurons analyzed by in vivo calcium imaging. PLoS One 9(8):e103321.
- Ohkura M, Sasaki T, Sadakari J, Gengyo-Ando K, Kagawa-Nagamura Y, Kobayashi C, and others. 2012. Genetically encoded green fluorescent Ca2+ indicators with improved detectability for neuronal Ca2+ signals. PLoS One 7(12):e51286.
- Orem BC, Rajaee A, Stirling DP. 2020. IP(3)R-mediated intra-axonal Ca(2+) release contributes to secondary axonal degeneration following contusive spinal cord injury. Neurobiol Dis 146:105123.
- Peng W, Wu Z, Song K, Zhang S, Li Y, Xu M. 2020. Regulation of sleep homeostasis mediator adenosine by basal forebrain glutamatergic neurons. Science 369(6508):eabb0556.
- Qian T, Wang H, Wang P, Geng L, Mei L, Osakada T, and others. 2023. A genetically encoded sensor measures temporal oxytocin release from different neuronal compartments. Nat Biotechnol 41(7):944–57.
- Ran C, Hoon MA, Chen X. 2016. The coding of cutaneous temperature in the spinal cord. Nat Neurosci 19(9):1201–9.
- Ran C, Kamalani GNA, Chen X. 2021. Modality-specific modulation of temperature representations in the spinal cord after injury. J Neurosci 41(39):8210–19.
- Rieder P, Gobbo D, Stopper G, Welle A, Damo E, Kirchhoff F, and others. 2022. Astrocytes and microglia exhibit cell-specific Ca(2+) signaling dynamics in the murine spinal cord. Front Mol Neurosci 15:840948.
- Roome CJ, Kuhn B. 2018. Simultaneous dendritic voltage and calcium imaging and somatic recording from Purkinje neurons in awake mice. Nat Commun 9(1):3388.
- Roome CJ, Kuhn B. 2020. Voltage imaging with ANNINE dyes and two-photon microscopy of Purkinje dendrites in awake mice. Neurosci Res 152:15–24.

Ropero Peláez FJ, Taniguchi S. 2016. The gate theory of pain revisited: modeling different pain conditions with a parsimonious neurocomputational model. Neural Plast 2016:4131395.

- Schmalbruch H. 1987. The number of neurons in dorsal root ganglia L4-L6 of the rat. Anat Rec 219(3):315–22.
- Sekiguchi KJ, Shekhtmeyster P, Merten K, Arena A, Cook D, Hoffman E, and others. 2016. Imaging large-scale cellular activity in spinal cord of freely behaving mice. Nat Commun 7:11450.
- Serebrovskaya EO, Podvalnaya NM, Dudenkova VV, Efremova AS, Gurskaya NG, Gorbachev DA, and others. 2020. Genetically encoded fluorescent sensor for poly-ADPribose. Int J Mol Sci 21(14):5004.
- Shaner NC, Lambert GG, Chammas A, Ni Y, Cranfill PJ, Baird MA, and others. 2013. A bright monomeric green fluorescent protein derived from Branchiostoma lanceolatum. Nat Methods 10(5):407–9.
- Shannonhouse J, Bernabucci M, Gomez R, Son H, Zhang Y, Ai CH, and others. 2022. Meclizine and metabotropic glutamate receptor agonists attenuate severe pain and Ca(2+) activity of primary sensory neurons in chemotherapy-induced peripheral neuropathy. J Neurosci 42(31):6020–37.
- Shekhtmeyster P, Carey EM, Duarte D, Ngo A, Gao G, Nelson NA, and others. 2023a. Multiplex translaminar imaging in the spinal cord of behaving mice. Nat Commun 14(1):1427.
- Shekhtmeyster P, Duarte D, Carey EM, Ngo A, Gao G, Olmstead JA, and others. 2023b. Trans-segmental imaging in the spinal cord of behaving mice. Nat Biotechnol 41(12):1729–33.
- Son H, Shannonhouse J, Zhang Y, Gomez R, Amarista F, Perez D, and others. 2024a. Elucidation of neuronal activity in mouse models of temporomandibular joint injury and inflammation by in vivo GCaMP Ca 2+ imaging of intact trigeminal ganglion neurons. Pain 165(12):2794–803.
- Son H, Zhang Y, Shannonhouse J, Gomez R, Kim YS. 2024b. PACAP38/mast-cell-specific receptor axis mediates repetitive stress-induced headache in mice. J Headache Pain 25(1):87.
- Son H, Zhang Y, Shannonhouse J, Ishida H, Gomez R, Kim YS. 2024c. Mast-cell-specific receptor mediates alcohol-withdrawal-associated headache in male mice. Neuron 112(1):113–23.e4.
- Sørensen B, Tandrup T, Koltzenburg M, Jakobsen J. 2003. No further loss of dorsal root ganglion cells after axotomy in p75 neurotrophin receptor knockout mice. J Comp Neurol 459(3):242–50.
- Subach OM, Sotskov VP, Plusnin VV, Gruzdeva AM, Barykina NV, Ivashkina OI, and others. 2020. Novel genetically encoded bright positive calcium indicator NCaMP7 based on the mNeonGreen fluorescent protein. Int J Mol Sci 21(5):1644.
- Sullivan SJ, Sdrulla AD. 2022. Excitatory and inhibitory neurons of the spinal cord superficial dorsal horn diverge in their somatosensory responses and plasticity in vivo. J Neurosci 42(10):1958–73.
- Sun F, Zhou J, Dai B, Qian T, Zeng J, Li X, and others. 2020. Next-generation GRAB sensors for monitoring dopaminergic activity in vivo. Nat Methods 17(11):1156–66.

- Sun L, Chen C, Xiang X, Guo S, Yang G. 2024. Generalized modality responses in primary sensory neurons of awake mice during the development of neuropathic pain. Front Neurosci 18:1368507.
- Tang P, Zhang Y, Chen C, Ji X, Ju F, Liu X, and others. 2015. In vivo two-photon imaging of axonal dieback, blood flow, and calcium influx with methylprednisolone therapy after spinal cord injury. Sci Rep 5:9691.
- Tian L, Hires SA, Mao T, Huber D, Chiappe ME, Chalasani SH, and others. 2009. Imaging neural activity in worms, flies and mice with improved GCaMP calcium indicators. Nat Methods 6(12):875–81.
- Turrini L, Ricci P, Sorelli M, de Vito G, Marchetti M, Vanzi F, and others. 2024. Two-photon all-optical neurophysiology for the dissection of larval zebrafish brain functional and effective connectivity. Commun Biol 7(1):1261.
- Villette V, Chavarha M, Dimov IK, Bradley J, Pradhan L, Mathieu B, and others. 2019. Ultrafast two-photon imaging of a high-gain voltage indicator in awake behaving mice. Cell 179(7):1590–608.e23.
- Wan J, Peng W, Li X, Qian T, Song K, Zeng J, and others. 2021. A genetically encoded sensor for measuring serotonin dynamics. Nat Neurosci 24(5):746–52.
- Wang F, Bélanger E, Côté SL, Desrosiers P, Prescott SA, Côté DC, and others. 2018. Sensory afferents use different coding strategies for heat and cold. Cell Rep 23(7):2001–13.
- Wang H, Fu Y, Zickmund P, Shi R, Cheng J-X. 2005. Coherent anti-Stokes Raman scattering imaging of axonal myelin in live spinal tissues. Biophys J 89(1):581–91.
- Wu A, Dvoryanchikov G, Pereira E, Chaudhari N, Roper SD. 2015. Breadth of tuning in taste afferent neurons varies with stimulus strength. Nat Commun 6:8171.
- Wu W, He Y, Chen Y, Fu Y, He S, Liu K, and others. 2024. In vivo imaging in mouse spinal cord reveals that microglia prevent degeneration of injured axons. Nat Commun 15(1):8837.
- Wu Z, Cui Y, Wang H, Wu H, Wan Y, Li B, and others. 2023. Neuronal activity-induced, equilibrative nucleoside transporter-dependent, somatodendritic adenosine release revealed by a GRAB sensor. Proc Natl Acad Sci U S A 120(14):e2212387120.
- Xu Q, Dong X. 2019. Calcium imaging approaches in investigation of pain mechanism in the spinal cord. Exp Neurol 317:129–32.
- Yarmolinsky DA, Peng Y, Pogorzala LA, Rutlin M, Hoon MA, Zuker CS. 2016. Coding and plasticity in the mammalian thermosensory system. Neuron 92(5):1079–92.
- Yoshihara K, Matsuda T, Kohro Y, Tozaki-Saitoh H, Inoue K, Tsuda M. 2018. Astrocytic Ca(2+) responses in the spinal dorsal horn by noxious stimuli to the skin. J Pharmacol Sci 137(1):101–4.
- Zeng J, Li X, Zhang R, Lv M, Wang Y, Tan K, and others. 2023. Local 5-HT signaling bi-directionally regulates the coincidence time window for associative learning. Neuron 111(7):1118–35.e5.
- Zhang S, Cai B, Li Z, Wang K, Bao L, Li C, and others. 2022. Fibroblastic SMOC2 suppresses mechanical nociception by inhibiting coupled activation of primary sensory neurons. J Neurosci 42(20):4069–86.

Zhao S, Cunha C, Zhang F, Liu Q, Gloss B, Deisseroth K, and others. 2008. Improved expression of halorhodopsin for light-induced silencing of neuronal activity. Brain Cell Biol 36(1–4):141–54.

- Zheng Q, Xie W, Lückemeyer DD, Lay M, Wang XW, Dong X, and others. 2022. Synchronized cluster firing, a distinct
- form of sensory neuron activation, drives spontaneous pain. Neuron 110(2):209-20.e6.
- Zhu W, Takeuchi S, Imai S, Terada T, Ueda T, Nasu Yand others. 2023. Chemigenetic indicators based on synthetic chelators and green fluorescent protein. Nat Chem Biol 19(1):38–44.